Surfaces and Interfaces 55 (2024) 105307

Contents lists available at ScienceDirect

Surfaces and Interfaces

journal homepage: www.sciencedirect.com/journal/surfaces-and-interfaces

The effect of ZnO nanoparticles morphology on the barrier and antibacterial properties of hybrid ZnO/graphene oxide/montmorillonite coatings for flexible packaging

Emre Alp [a,†], Federico Olivieri [b,†], Martina Aulitto [c], Rachele Castaldo [b,*], Patrizia Contursi [c], Mariacristina Cocca [b], Gennaro Gentile [b]

[a] Metallurgy and Materials Engineering Department, Faculty of Engineering, Architecture and Design, Kutlubeyyazıcılar Campus, 74110 Center/Bartin, Turkey
[b] Institute for Polymers Composites and Biomaterials, National Research Council of Italy, Via Campi Flegrei 34, 80078 Pozzuoli, Italy
[c] Department of Biology, Università degli Studi di Napoli Federico II, 80138 Napoli, Italy

ARTICLE INFO

Keywords:
Zinc oxide
Graphene oxide
Montmorillonite
Oxygen barrier
Antimicrobial activity
Coatings

ABSTRACT

The need for eco-friendly packaging solutions is continuously increasing, with several materials being investigated to develop functional coatings able to contrast food degradation due to oxidation and bacterial growth. In this work, ZnO nanoparticles (NPs) with various morphology and size from spherical to hexagonal, dots-like and platelets-like shape, were synthesized. Hybrid coatings constituted by ZnO NPs, graphene oxide (GO) and montmorillonite (MMT) were applied onto flexible polyethylene (PE) in order to exploit the 2D nanomaterials self-assembly ability and gas barrier properties and to synergistically combine these functionalities with the antibacterial activity of ZnO. The effect of ZnO NPs morphology and the ZnO/GO/MMT relative content was explored to obtain nanostructured coatings with optimized functionality. Results evidence a correlation between oxygen permeability and microbial proliferation, allowing to reach 88 % of reduction of PE oxygen permeability and about 60 % inhibition towards Gram-positive (i.e. *Weizmannia coagulans*) and Gram-negative (i.e. *Escherichia coli*) microorganisms.

1. Introduction

Facing with a burgeoning global population, ensuring a secure and sustainable food supply has become of paramount importance. This challenge is further powered by the escalating concerns surrounding food waste, environmental impact, and consumer safety. In this context, the development of innovative and effective food packaging solutions has emerged as a critical area of research [1–4]. Conventional food packaging materials, primarily polymers, have played a significant role in preserving food quality and extending shelf life. Plastic products exhibit significant design flexibility, are heat sealable, easy-to-print, chemically inert, lightweight and inexpensive; these are very appealing skills for food packaging applications. Despite these advantages, the main weakness of several plastic products is their permeability to gases, vapours, and light, since oxygen and light are the main issues for most food deterioration processes.

Multilayer packaging with different coupled polymer layers or alternated with aluminium layers, have shown excellent results for the improvement of barrier properties against gases and light. Nevertheless, these solutions impede the recyclability of the plastics, representing a serious issue for their end-of-life [5]. For this reason, the realization of recyclable polymer-based products with enhanced gas and light barrier properties is a research topic whose industrial interest is continuously growing in the last years. As an alternative to the traditional approaches, recently, nanostructured coatings have acquired high relevance [6]. Indeed, by proper design, the confinement of the nanoparticles on the external surface of the packaging serves multiple advantages: i) lowering the amount of nanomaterial, ii) preserving the thermo-mechanical properties and the processability of the polymer films and iii) imparting additional properties to the treated surface, such as antimicrobial and antibacterial properties [7,8]. Moreover, due to the very limited amount of functional fillers applied as coatings, systems realized by this approach can be considered *monomaterial* packaging, and the functional coatings do not compromise the recyclability of plastics,

* Corresponding author.
E-mail addresses: rachele.castaldo@cnr.it, rachele.castaldo@ipcb.cnr.it (R. Castaldo).
† These authors contributed equally to this work.

https://doi.org/10.1016/j.surfin.2024.105307
Received 21 June 2024; Received in revised form 16 October 2024; Accepted 20 October 2024
Available online 21 October 2024

representing an interesting solution in the context of circular economy [9]. Fucntional coating for packaging applications can be developed by rod coating techniques [9], spin coating [10], layer-by-layer techniques [11].

Due to their high aspect ratio, different 2D nanomaterials have been tested for gas barrier applications. In particular, graphene oxide (GO) has been largely exploited through its engineering in purposely tailored microscopic and macroscopic structure. In fact, GO is easily dispersible in water and self-assembles on diverse substrates, guided by direct water evaporation or freeze-drying, producing thin films and porous 3D networks [12–14]. Different GO self-assembled structures are largely investigated in order to exploit their barrier and adsorption properties [13–15].

Lamellar nanoparticles deriving from phyllosilicates have also exhibited high potential as effective barrier agents when arranged in well orientated nanostructures. For example, hybrid coatings based on GO and montmorillonite (MMT) showed interesting performances as barrier coatings for monomaterial flexible packaging, being able to significantly reduce the oxygen transmission rate of polyolefins without affecting their recyclability [9].

Antimicrobial efficiency is another important concept in food packaging considering the growth control of microorganisms that cause foodborne illnesses. Bare plastic films do not possess any antimicrobial activity against the growth of microorganisms in the packed food. Zinc oxide (ZnO) nanoparticles (NPs) have garnered considerable attention in the realm of food packaging [16], offering a range of advantages over conventional packaging materials, making them a promising alternative for the future [17]. Firstly, ZnO NPs exhibit broad-spectrum antimicrobial activity against a diverse array of foodborne pathogens, including bacteria, fungi, and viruses [18]. This property is attributed to the release of zinc ions (Zn^{2+}) from the NPs, which disrupt the cell membranes of microorganisms, leading to their inactivation [19]. The antimicrobial efficacy of ZnO NPs is influenced by many factors such as their size, shape, concentration, and surface modification [20–22]. To impart antibacterial behavior to packaging films, two prevalent methods can be used: the first involves the deposition of antimicrobial substance onto plastic surface and the second is based on the embedding of the active agents within the polymer matrix [23]. Also in this case, the application of functional agents as surface coatings is gaining an ever-increasing attention for the possibility of limiting the amount of nanomaterials needed to impart the target property. Moreover, ZnO, thanks to its wide bandgap, possess exceptional ultraviolet (UV) light blocking capabilities, enabling them to protect light-sensitive food products from degradation and discoloration [24], preventing the formation of off-flavors and the loss of nutrients. They also display photocatalytic activity, meaning that they can generate reactive oxygen species (ROS) when exposed to UV light [25,26]. Therefore, since ROS can break down organic molecules, ZnO NPs have been recently tested as photocatalysts for the degradation of plastics and microplastics waste in aqueous environment [26,27] and as active particles in self-cleaning and antifouling coatings [28]. Additionally, ZnO NPs can effectively enhance the barrier properties of packaging materials, reducing their permeability to gases (such as oxygen and carbon dioxide), and moisture [29]. Moreover, multifunctional nanocomposites containing GO and ZnO exhibited excellent water vapor barrier, UV-light barrier and antimicrobial properties, pointing to their high potential in food packaging applications [30-32]. For all these reasons, the incorporation of ZnO NPs into food packaging materials offers a promising approach to address the challenges associated with food preservation and safety.

In this work, ZnO NPs were synthesized through hydrothermal and solvothermal methods in order to obtain different nanoparticles with various morphology and size. After a thorough characterization of ZnO NPs morphology, structure and specific surface area, flexible thin coatings containing ZnO NPs were realized by combining them with 2D nanostructured materials such as GO and MMT. The self-assembly ability of GO and GO/MMT hybrids was exploited to embed ZnO NPs into bi-component and three-component hybrid coatings obtained by deposition, via rod coating, of hybrid aqueous dispersions of the nanomaterials onto flexible polyethylene (PE) films. Finally, the effect of the different morphology of the ZnO NPs on the coatings morphology, oxygen permeability and antibacterial properties was evaluated.

2. Experimental section

2.1. Materials

Zinc nitrate hexahydrate ($Zn(NO_3)_2{\cdot}6H_2O$), zinc acetate dihydrate ($Zn(CH_3CO_2)_2{\cdot}2H_2O$), polyvinylpyrrolidone (PVP, average mol wt 40,000), sodium dodecyl sulfate (SDS), sodium hydroxide (NaOH), ascorbic acid (AA) were purchased by Sigma Aldrich.

Graphene oxide (GO) water dispersion (4.0 mg/mL, flake size 1–6 μm, D50 = 4 μm) was purchased from Nanesa S.r.l. (Arezzo, Italy). Cloisite Na^+ (MMT) was purchased from BYK Additives & Instruments (Wesel, Germany). All chemicals used in the experimental process were of analytical grade and used without any further purification.

Polyethylene flexible films (PE, thickness 60 μm, corona treated, with a surface tension > 38 dyne/cm) were kindly supplied by Flex Packaging AL S.p.A. (Cava de' Tirreni, Italy).

2.2. Zinc oxide nanoparticles synthesis

Three types of ZnO NPs were synthesized by hydrothermal method, while a fourth one was prepared by solvothermal synthesis in atmospheric conditions.

For the hydrothermal synthesis, a 100 mL Teflon-lined stainless-steel autoclave was used. Using this approach, the precursors were dissolved in 50 mL of ultrapure water and stirred until a homogeneous solution was obtained. For the three type of ZnO NPs reagents were added as herein detailed: i) 1.5 g of $Zn(NO_3)_2{\cdot}6H_2O$ and 1 g of PVP were dissolved in 50 mL of water and 1 mL of NaOH solution (2.4 g NaOH/20 mL) was added into that solution; ii) 1.5 g of $Zn(NO_3)_2{\cdot}6H_2O$ and 1 g of PVP were dissolved in 50 mL water and 2 ml of NaOH solution (2.4 g NaOH/20 mL) were added into that solution; iii) 1.5 g of $Zn(NO_3)_2{\cdot}6H_2O$ and 1 g of SDS were dissolved in 50 mL of water and 1 g of NaOH solution was added into the former solution. Afterwards, they were quickly transferred to a Teflon-lined stainless-steel autoclave. The autoclave was heated up to 120 °C and kept at this temperature for 12 h. After the hydrothermal process, synthesis products were centrifuged and washed with distilled water and ethanol several times to remove residual products. Finally, the washed nanoparticles were dried in oven at 65 °C overnight.

The fourth type of ZnO NPs was synthesized under atmospheric conditions. 2 g of $Zn(CH_3CO_2)_2{\cdot}2H_2O$, 1.55 g of NaOH and 1.0 g of AA were dissolved in 80 mL water. The obtained solution was stirred magnetically at 80 °C for 1 h. Synthesis products were purified with distilled water and ethanol as described above for the hydrothermal synthesis products and the resulting nanoparticles were dried in oven at 65 °C overnight.

2.3. Zinc oxide nanoparticles characterization

ZnO NPs morphology was analysed by field emission gun scanning electron microscope (SEM) and by transmission electron microscopy (TEM). SEM analysis was performed by using a TESCAN™ MAIA XMU (Brno, CZ). Before analysis, ZnO NPs were deposed onto SEM stubs. TEM analysis were performed using an FEI Tecnai G12 Spirit Twin (LaB_6 source) at 120 kV acceleration voltage (FEI, Eindhoven, the Netherlands). TEM images were collected on an FEI Eagle 4 k CCD camera. Before the analysis, nanoparticles were dispersed in distilled water through sonication using a Sonics Vibracell (Newtown, CT, USA) ultrasonic processor (500 W, 20 kHz) at 25% of amplitude for 5 min and then collected on carbon-coated copper grids.

X-Ray analysis of the ZnO NPs was performed by using a X-ray diffractometer (XRD) with Cu Kα radiation by RIGAKU SmartLab™ (Tokyo, JPN).

Specific surface area (SSA) was evaluated by nitrogen adsorption analysis, performed by means of a 3Flex adsorption analyser (Micromeritics, Norcross, GA, USA). N_2 adsorption/desorption isotherms were recorded at 77 K and SSA was determined from the linear part of the Brunauer−Emmett−Teller (BET) equation. Before analysis, the ZnO NPs were degassed at 150 °C for 10 h under vacuum ($P < 10^{-7}$ mbar). Measurements were performed using high-purity gases (>99.999%).

2.4. Nanostructured hybrid coatings deposition

ZnO NPs and MMT dispersions in water at 4.0 mg/mL were prepared by ultrasonication at 25% of amplitude (500 W, 20 kHz) for 30 min, with 30 s/30 s on/off cycles using a Sonics Vibracell ultrasonicator processor (Newton, CT, USA). Then, proper amounts of the ZnO NPs dispersion were mixed with the GO dispersion in the 75/25 and 50/50 ZnO/GO volume ratios and ternary mixtures in which ZnO NPs, GO and MMT dispersions were mixed in the 30/30/40 ZnO/GO/MMT volume ratio were prepared. The ZnO/GO and ZnO/GO/MMT dispersions were ultrasonicated for 10 min using the same conditions as described above.

The ZnO/GO and ZnO/GO/MMT dispersions were deposited on PE films by rod coating depositing wet films of 100 μm. For comparison, a plain GO coating and a GO/MMT coating with the GO/MMT 57/43 vol ratio (mimicking the GO/MMT ratio in ternary coatings without the ZnO component) were realized.

2.5. Nanostructured hybrid coatings characterization

Static contact angles (CA) of the GO, GO/MMT, ZnO/GO and ZnO/GO/MMT dispersions on PE was evaluated with a FTA 1000 (First Ten Ångstroms) instrument. 10 μL drops of the nanoparticles dispersions were positioned on the film surface, the images were captured and the CA were geometrically evaluated with the instrument software as the angle formed by the solid surface and the tangent to the droplet. Each measurement was repeated on six different areas of the sample. The experiments were conducted at room temperature.

ZnO/GO/MMT coated PE samples were characterized by scanning electron microscopy (SEM). The analyses were performed using a FEI Quanta 200 FEG SEM (Eindhoven, The Netherlands) with a secondary electron detector and an acceleration voltage of 10–30 kV. Before the analysis the samples were sputter coated with gold/palladium.

Oxygen permeability measurements were performed on all PE coated samples and on PE as a reference at 25 °C and 50% RH using a Multiperm Extrasolution Permeabilimeter (Capannori, IT). Before the analysis the films were conditioned with nitrogen. All gases used were high purity gases (99.9999%). The results, representing the average value of three replicates, were expressed as the Oxygen Transmission Rate (OTR, cm^3/m^2 24 h at one atmosphere pressure difference).

Antimicrobial activity of ZnO/GO/MMT PE coated films was assessed as follows. Glycerol stock cultures of bacterial strains *E. coli* Rosetta™ DE3 pLYS and *W. coagulans MA-13* [33] were stored in 30% glycerol at −80 °C. The strains were cultivated in Luria Bertani (LB) medium at 37 °C with constant agitation at 180 rpm for 16 h All the PE coated samples and plain PE as a reference were cut into 2.5 cm x 2.5 cm squares and then submerged into 1 mL of the diluted cells (× 10^5 cells/mL) in 6-well Petri dishes. Next, the samples were covered using sterilized polyethylene films and maintained at 37 °C in static conditions. Turbidity of the cell suspension, as a measure of bacteria growth, was recorded spectrophotometrically at 600 nm using a microplate reader (Synergy H4; Bio-TEK Instruments, Winooski, VT, USA) (Synergy) after 16 h To counteract potential interference during optical measurements, the same liquid medium devoid of microorganisms but containing an identical amount of the PE coated samples and the bacterial cultures devoid of the films ~~under study~~ were used as negative and positive controls, respectively.. All experiments were conducted in triplicates.

Inductively Coupled Plasma Mass Spectroscopy (ICP-MS) was used to measure the content of Zn^{+2} by following a previously reported Standard Operating Procedure [34]. All samples are filtered in the field through a 0.22 μm filter and diluted prior to analysis In order to reduce the dissolved solid.

3. Results and discussion

3.1. Zinc oxide nanoparticles

The morphological features of the as-synthesized ZnO NPs were characterized by SEM and TEM analysis (Fig. 1), wherein the NPs show a highly homogeneously monodispersed shape. The NPs synthesized by using PVP as a surfactant and by adding 1 mL NaOH solution to the reaction media are in the form of hexagonal cylinders (coded as ZnO—H) whose height is 129 ± 13 nm and edges are 107 ± 12 nm, as shown in Fig. 1a,b. The NPs in Fig. 1c,d, synthesized by using PVP and with higher amount of NaOH solution (2 mL), are polyhedral-like and with an approximation to a spherical shape their average diameter is 69 ± 8 nm (coded as ZnO-S). NPs synthesized by using SDS as a surfactant have a platelet shape (coded as ZnO-P); their average dimensions are 387 ± 95 nm in length, 170 ± 23 nm in width and 27 ± 9 nm in thickness, as shown in Fig. 1e,f. NPs synthesized in atmospheric conditions (Fig. 1g,h) without high pressure (coded as ZnO-D, for "dots") have spherical-like form but smaller than ZnO-S and diameters ranging from 10 to 30 nm.

Structural analysis of the synthesized particles was performed by XRD, and their characteristic patterns are presented in Fig. 2a. All the obtained diffraction patterns of the synthesized NPs are consistent with the International Centre for Diffraction Data (ICCD) file data. All the peaks in the XRD pattern are indexed as the wurtzite ZnO phase (space 185 group: P63mc) with lattice parameters of $a = 0.3298$ nm and $c = 0.5206$ nm (PDF Card No.: 00–036–1451). The strong diffraction patterns with narrow peaks indicate that the synthesized ZnO NPs have high crystallinity. No diffraction peaks apart from those of the wurtzite ZnO phase were observed, which indicates that no impurities were detected, regardless of the synthetic conditions and the selected stabilizing agents.

Nitrogen adsorption/desorption isotherms of ZnO NPs are shown in Fig. 2b and BET surface area values are reported in Table 1. Compared to the other NPs, the smaller ones, ZnO-D, exhibit the greatest nitrogen adsorption capacity, coherently with their higher surface area, of about 28 m^2/g. Then, spherical NPs, ZnO-S, characterized by higher size with respect to ZnO-D, exhibit BET SSA of about 11 m^2/g. Finally, platelet-shape ZnO-P and hexagonal NPs ZnO—H show BET SSA of about 9 m^2/g and 4 m^2/g, respectively. It is worth to note that even if platelet-shaped NPs show bigger lateral size (up to 500 nm) than the hexagonal ZnO—H (about 110 nm), ZnO-P NPs are characterized by moderate thickness (about 55 nm) with respect to ZnO—H (about 125 nm) and, therefore, they ultimately show higher SSA.

3.2. Nanostructured hybrid coatings

ZnO/GO/MMT hybrid coatings were realized by rod coating, a largely employed technique to obtain thin coating on various substrates with controllable thickness and allowing to cover large areas [9,35-37]. To fully exploit this technique, a good wettability of the solution or dispersion to be deposed on the substrate is a positive premise. Moreover, for nanoparticles dispersion, the nanoparticles should be characterized by good self-assembly properties, allowing to obtain continuous and homogeneous coatings. While each type of ZnO NPs dispersed in water and deposed on polymer substrates do not form a continuous film, the mixing of these NPs even with a small amount of GO dispersion (ZnO:GO = 75:25 wt/wt) allows to obtain, by rod coating, continuous

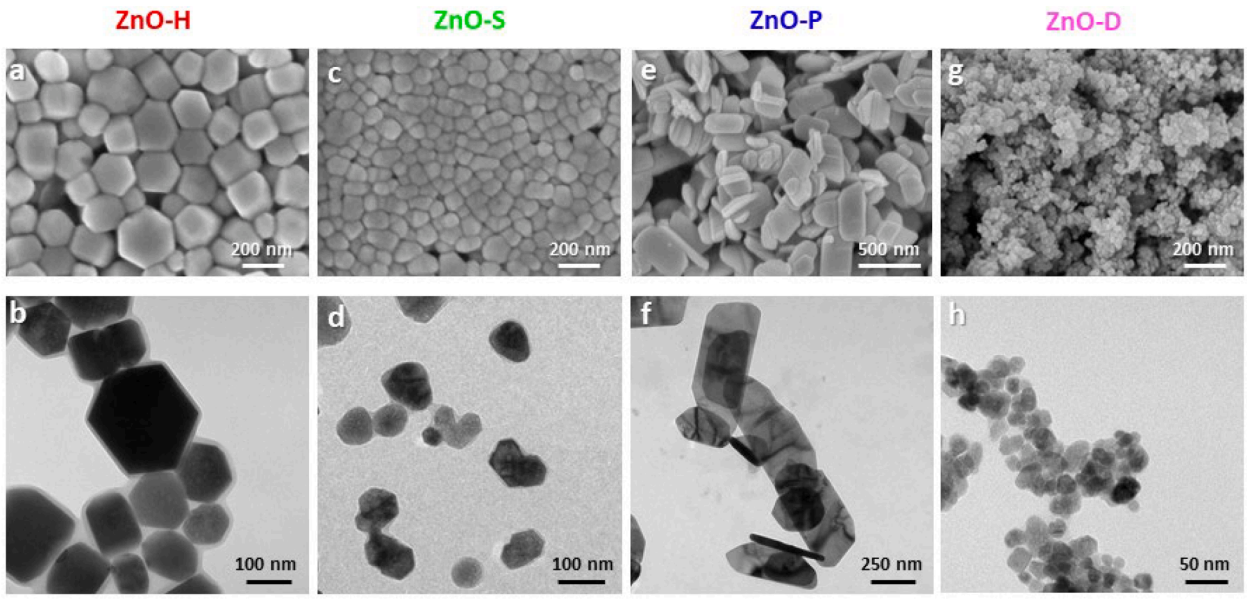

Fig. 1. SEM (a, c, e, g) and TEM (b, d, f, h) images of the synthesized ZnO nanoparticles: a-b) ZnO—H (hexagons), c-d) ZnO-S (spheres), e-f) ZnO-P (platelets), g-h) ZnO-D (dots).

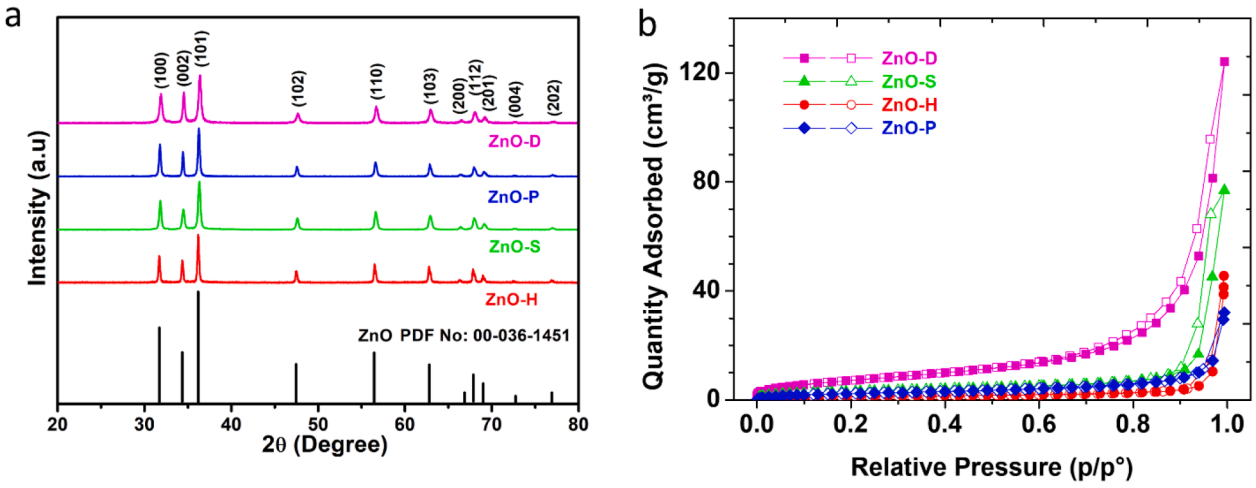

Fig. 2. X-Ray Diffraction patterns (a) and nitrogen adsorption/desorption isotherms (b) of the ZnO nanoparticles.

Table 1
BET SSA of ZnO NPs.

Sample	BET specific surface area (m^2/g)
ZnO-D	27.8 ± 0.14
ZnO-S	11.3 ± 0.07
ZnO—H	4.39 ± 0.03
ZnO-P	8.88 ± 0.08

hybrid coatings on PE of nominal thickness of 200 nm (Fig. 3a shows the ZnO-P75_GO25 coating).

GO, indeed, is largely known for its self-assembly properties [13], also in presence of other lamellar nanoparticles such as MMT [15]. Even if the GO dispersion does not show very low contact angle values on PE (80.5° ± 4.3°, see Fig. 4), by spreading the dispersion through rod coating, a very uniform surface is obtained. Then, the addition of ZnO, MMT dispersion or both of them to the GO one allows to obtain lower contact angle values, of 76.7° ± 3.2° for the GO/MMT dispersion, comprehended between 79.8° ± 3.5° and 81.9° ± 3.7° for ZnO/GO 50/50 dispersions, between 75.6° ± 3.1° and 77.1° ± 2.3° for ZnO/GO 75/25 dispersions and between 66.2° ± 3.5° and 68.2° ± 2.9° for ZnO/GO/MMT 30/30/40 dispersions, with very low variations depending on the ZnO nanoparticle type (Fig. 4). Also in this cases, even if the contact angle of the dispersions are not very low, all samples are in the range of hydrophilicity, and through spreading of the dispersions via rod coating, continuous coatings are obtained (examples in Fig. 3). In particular, in comparison to ZnO/GO coatings containing 75 wt% of ZnO, ZnO/GO coatings obtained with the 50:50 wt/wt composition are characterized by a browner coloration, due to the higher amount of GO phase, as shown in Fig. 3, in which the coatings realized with the ZnO-P NPs are reported. Finally, three-component coatings containing MMT were realized in the ZnO/GO/MMT 30:30:40 by weight composition. These latter have the most homogenous morphology as evidenced by visual inspection (Fig. 3c). In all cases, the thin coating does not affect the flexibility of the polymer substrate and appears well-adhered to the PE, as demonstrate by the absence of detachment or irregularities, as shown on a bent film in Fig. 3d.

SEM images of the bi- and three-component coatings, in comparison to plain GO and GO-MMT coatings, are shown in Fig. 5.

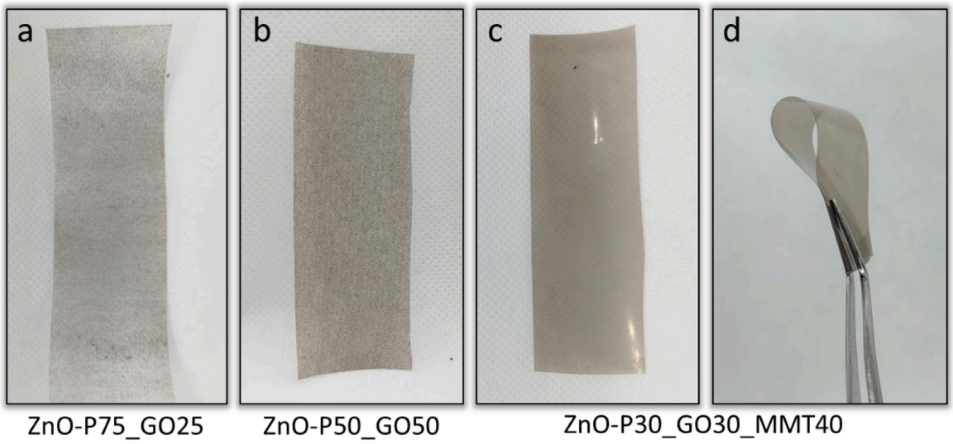

Fig. 3. Images of ZnO-P/GO/MMT coatings at various composition: ZnO:GO = 75:25 (a), ZnO:GO = 50:50 (b) and ZnO:GO:MMT = 30:30:40 (c, d).

Fig. 4. Water contact angle images and values of GO, GO/MMT, ZnO/GO and ZnO/GO/MMT dispersions on PE.

While plain GO coating shows a homogenous morphology characterized only by the typical wrinkles due to the overlapping of the GO platelets, the bi-component coatings exhibit some segregation phenomena, demonstrated by the evidence of diffuse nanometric particles, slightly evident in the GO_MMT coating and clearer in ZnO/GO coatings, due to the lamellar nature of MMT. The aggregated NPs are also present in the three-component coatings; however, these latter present a smoother morphology and higher homogeneity with respect to the corresponding bi-component ones, in accordance with their more homogeneous morphology noticed by visual inspection. That is probably due to the good interaction between the two ceramic phases, ZnO and clay [38], able to improve the dispersion of ZnO in the hybrid GO/MMT phase.

Results of oxygen permeability tests (Fig. 6) are consistently in line with the morphology of the coatings. While GO coating shows the highest OTR reduction, down to values of 150 $cm^3/(m^2 \cdot 24\ h)$, the presence of a second phase such as MMT or ZnO NPs lowers the barrier effect to oxygen (OTR 707 $cm^3/(m^2 \cdot 24\ h)$). In particular, upon exfoliation in water, while the MMT platelets are able to intercalate with GO into an hybrid layered nanostructure [15], the ZnO NPs, due to their particle nature, although well dispersed into the GO phase, may represent possible defect points in the thin coatings which affect the oxygen barrier properties of the samples. Indeed, the samples coated with 75% of ZnO NPs and 25% of GO show higher OTR values (1700–2000

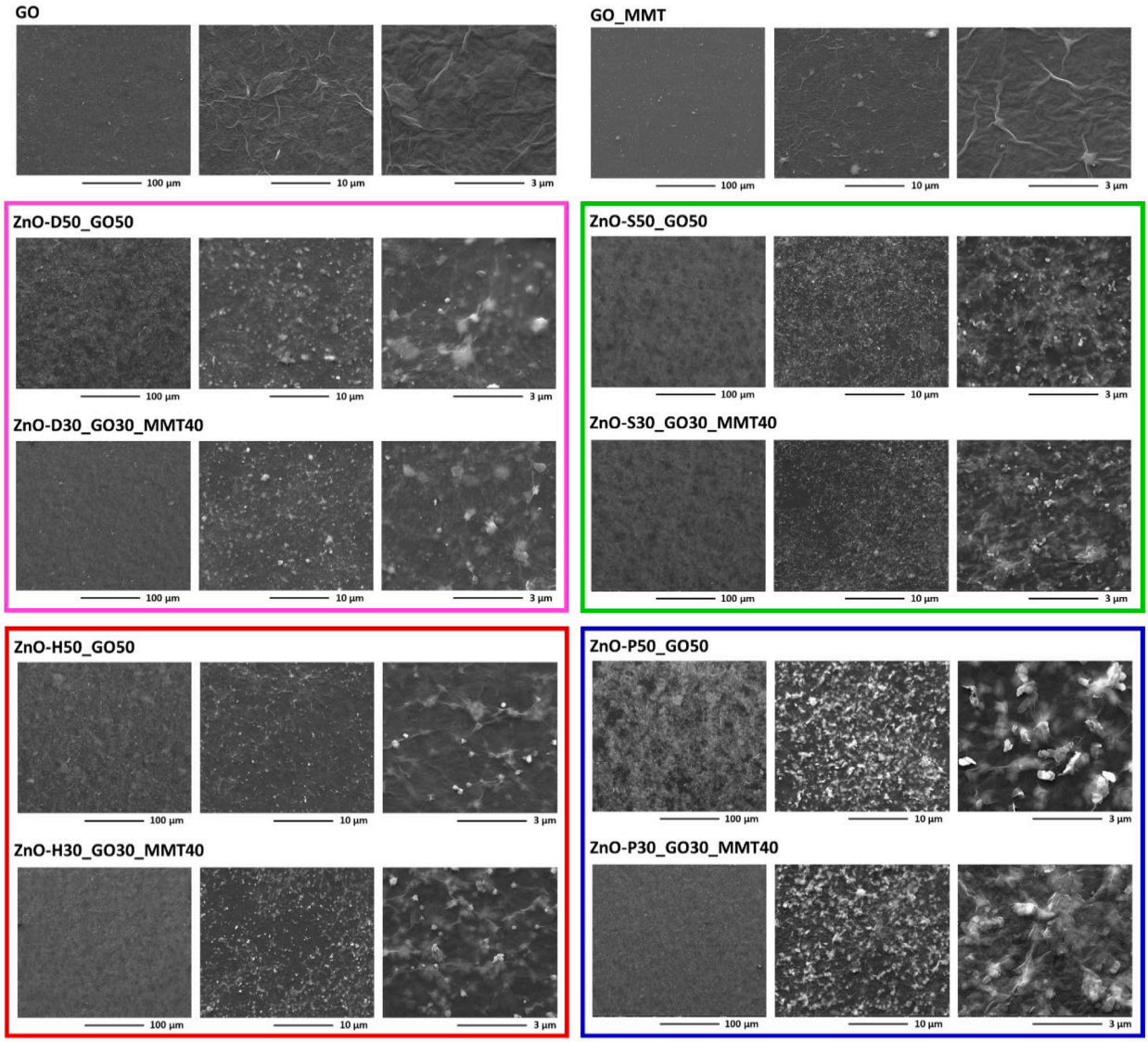

Fig. 5. SEM images of GO, GO_MMT and ZnO/GO/MMT hybrid coatings.

$cm^3/(m^2 \cdot 24\ h)$) than the corresponding coatings composed of 50% ZnO NPs and 50% of GO (583–1039 $cm^3/(m^2 \cdot 24\ h)$). Then, in all cases, the presence of MMT in the three-component coatings favors the realization of higher barrier coatings, in agreement with their homogenous morphologies. Indeed, the relative OTR values range between 554 $cm^3/(m^2 \cdot 24\ h)$ for the coating containing the dot-shaped nanoparticles, ZnO-D, and 233 $cm^3/(m^2 \cdot 24\ h)$ for the platelets-shaped ZnO-P NPs filled coating.

It is worth to note that the coating obtained with the ZnO-P NPs reaches OTR values comparable to those of the plain GO coating, achieving 88% of OTR reduction with respect to the pristine PE film and therefore representing a valid alternative to GO coatings for oxygen barrier applications. This may be ascribable to the flattened shape of these nanoparticles, which offer, in the three-component coating, the highest resistance to the O_2 path.

The antibacterial activity of the nanostructured hybrid coatings towards two bacterial strains was investigated. The microorganisms chosen for these experiments are widely distributed across both the human body and natural surroundings. *Weizmannia coagulans*, a Gram- and catalase-positive bacterium, stands out due to its spore-forming ability. This bacterium is commonly found in various environments, including food, soil and water ecosystems and resides in the gastrointestinal tracts of humans and animals. Specifically, the *W. coagulans* strain used in this work (MA-13) was isolated from bean processing waste [39,40]. In contrast, *Escherichia coli* is a Gram-negative bacterium that is a member of the *Enterobacteriaceae* family. While many *E. coli* strains are harmless and even beneficial to the human body, others can be pathogenic and cause a range of health issues. In this study, the efficiency, and the synergistic effect among ZnO, GO and MMT were evaluated in regards of antimicrobial activity and shown in Fig. 7.

Values laying underneath the threshold of 50% inhibition are considered as clearly antibacterial outcomes. Compared to control samples (plain PE, PE coated with GO and GO/MMT), most of the hybrid coatings exhibit an antibacterial effect on both strains, with an enhanced effect on *W. coagulans*. Indeed, the percentage of growth inhibition is exerted by all the hybrid coatings with ZnO-D50_GO50 being the most (% inhibition about 61%) and Zn-S50_GO50 less effective (% inhibition about 37%). This result indicates that the antibacterial activity is affected by the microstructural features of ZnO NPs. A similar and overlapping trend is observed for ZnO-P50_GO50 which is more effective on *E. coli* (% inhibition 74%) than on *W. coagulans* (% inhibition 48%). Noteworthy the effect of ZnO-D50_GO50 on *E.coli* is negligible, despite being the most effective on *W. coagulans*. Moreover, ZnO-P30_GO30_MMT40 has an identical effect on both strains and

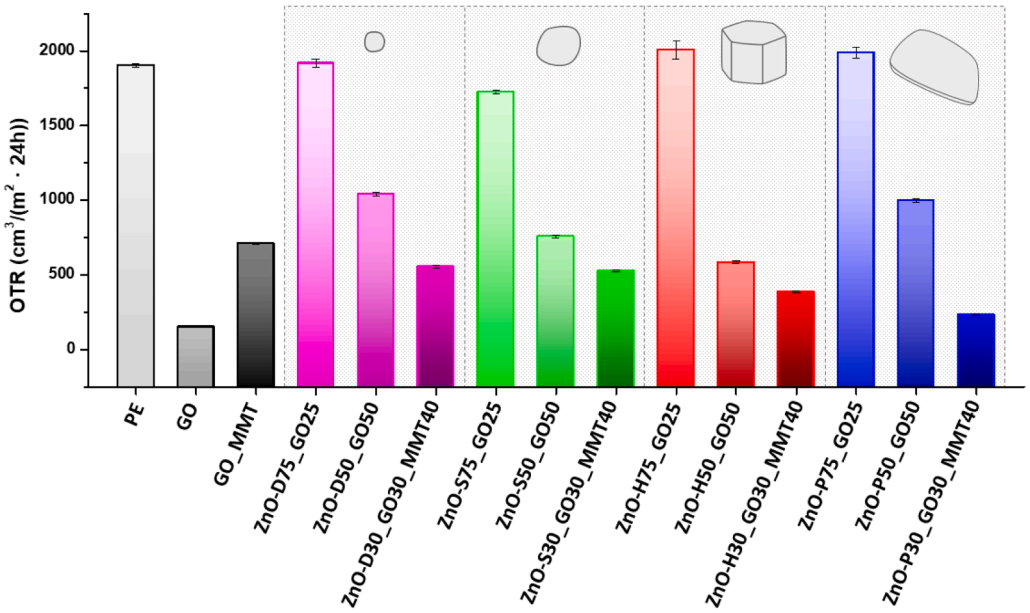

Fig. 6. OTR values of plain PE and PE coated with GO, GO/MMT and ZnO/GO/MMT at 25 °C and 50% RH.

therefore can be considered as a wide-spectrum antimicrobial nanostructured coating. Since ZnO-P30_GO30_MMT40 has the lowest OTR value, it is expected that the reduction of the oxygen diffusion might have a positive effect on slowing down the proliferation of obligatory aerobic bacteria [41]. In general, the antibacterial effect correlates with the ZnO percentage in the hybrid coatings probably as a consequence of the increased local concentration of ZnO in the bi-components compared to the three-components nanomaterial.

The reason for which the shape of nanoparticles influences the differential antibacterial effect towards the two strains is not easy to rationalize. Therefore, metal ions analysis through ICP-MS was carried out to evaluate the release of Zn^{2+} in solution. In particular, ZnO-D50_GO50, ZnO-P50_GO50 and ZnO-P30_GO30_MMT40 coatings were selected since they exhibit significant activity towards *E.coli*, and *W. coagulans* or both. In all the cases, a small amount of Zn^{2+} was detected (about 0.6–1.5 mg/ml), suggesting that the antibacterial effect can be traced back to direct interaction of Zn^{2+} through electrostatic forces at the surface level, damaging/deconstructing cell membrane or generating hydrogen peroxide upon its internalization [42,43]. However, despite the coatings are designed to be applied on the external side of the packaging, without entering in direct contact with food, it is to be remarked that the level of Zn^{2+}released is lower than that indicated in the EFSA (European Food Safety Authority 12.7 mg/day for women and 16.3 mg/day for men) guidelines on maximum zinc level allowed in feed and food applications [44].

3.3. Comparison with literature

ZnO NPs have been largely employed in nanocomposite systems to exert their renowned antibacterial activity [45], also combined to other nanostructured materials, such as GO, to induce also barrier properties to the nanocomposite [46]. A direct comparison of performances of the hybrid ZnO/GO/MMT coatings reported in this work with literature data is hard because each system reported in literature is not always analyzed in terms of both oxygen permeability and antimicrobial properties.

For example, poly(lactic acid) (PLA)/ZnO NPs composite films were prepared by solvent casting, tested for water vapour permeability (WVP) and antimicrobial activity but not tested for oxygen permability. E. Coli cell viability was about halved in 12 h by the film containing 1.5 wt% NPs and water vapour permeability (WVP) was reduced up to about 30% with the film containing 0.5 wt% NPs, with respect to the plain PLA films [45]. Liew et al. [46] also prepared by solvent casting PLA nanocomposite films containing ZnO NPs and GO. Also in this case oxygen permeability tests were not reported. They obtained a 46% reduction of WVP and a 67.98 % reduction rate of E. Coli with the PLA film containing 1.11 wt% GO and 1.25 wt% ZnO NPs, with respect to plain PLA. Channa et al. prepared polyvinyl alcohol (PVA) nanocomposite films with ZnO NPs for packaging application showing the effectiveness of ZnO NPs as UV blocking material and as protecting agent against oxidation. Films containing 0.8 wt% of ZnO NPs showed a reduction of WVTR of about 4 times with respect to plain PVA films but no significant effect on oxygen permeability [47].

Coatings containing ZnO were developed with different techniques but only tested for their antimicrobial activity. Rokbani et al. developed ZnO coatings on low density polyethylene (LDPE) films by spreading ZnO NPs at the exit of a cast film die following extrusion of LDPE [48]. Obtaining a homogeneous morphology was challenging in this setup, but they obtained good antimicrobial effect against E. Coli bacteria: the E. coli population was completely eradicated, in comparison to control samples. More homogenous coatings were obtained by sputtering techniques on different polymer substrates, such as PLA and polyethylene terephthalate (PET). Valerini et al. realized Al doped ZnO coatings on PLA by sputtering a ZnO/Al_2O_3 target at different power up to 200 W and tested their antimicrobial activity against E. Coli [49]. The number of colony forming units (CFU) strongly decreases in all the experiments in presence of the coated polymer, with respect to the control PLA after 2.5 h of incubation. Carvalho et al. [50] developed ZnO coatings on PET by reactive magnetron sputtering obtaining coating with variable thickness from 50 nm to 600 nm. They evaluated the films antibacterial activity against E. Coli; starting from coating with thickness of 200 nm, the cells were halved in the stationary phase with respect to the control PET film. With another approach, nanocomposite coatings based on chitosan and ZnO NPs deposed on PE were developed [51]. These coatings showed complete inhibition of the incubation of both Gram-positive and Gram-negative bacteria. In this case, the antimicrobial effect is also to attribute to the chitosan phase, whose antimicrobial activity is due to its positively charged amine groups forming electrostatic interactions with anionic groups of microbial cell membranes. However, the antimicrobial effect of chitosan coatings diminishes over time, and is improved and prolonged by the addition of ZnO NPs.

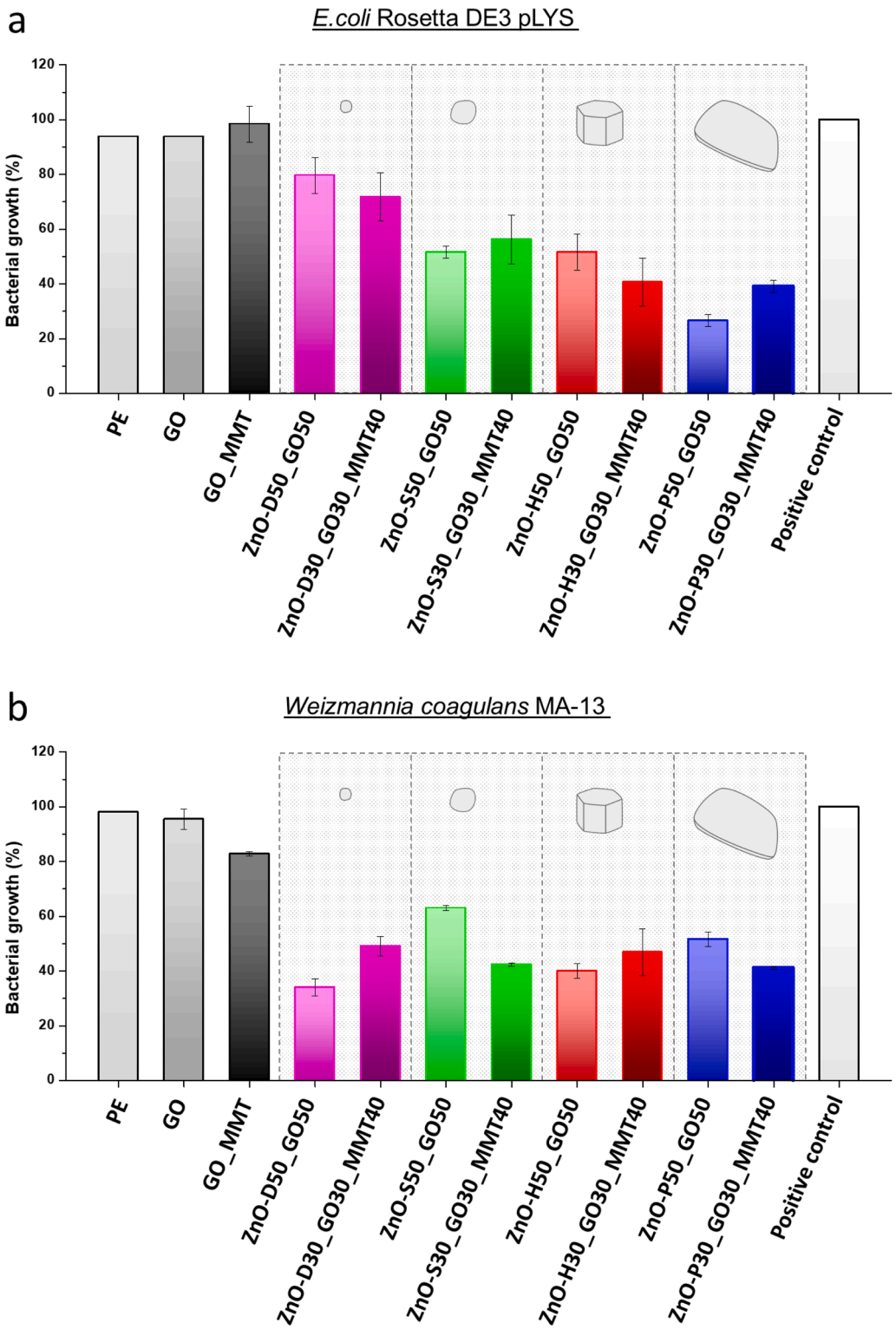

Fig. 7. Antimicrobial activity of PE and PE coated with GO, GO/MMT and ZnO/GO/MMT. Data are presented as mean ± of three independent experiments, each performed in biological duplicates.

Compared to literature data reported in the above systems, the hybrid ZnO/GO/MMT coatings realized in this work are very interesting if considered the versatility of the applicability of these coatings and the synergistic effect among GO, MMT and ZnO NPs in the obtained multifunctional coating, characterized by both oxygen barrier properties and antimicrobial activity. The bi- and three-component thin (200 nm) coatings realized in this study containing GO, MMT and ZnO NPs of tailored shape and size have very homogeneous morphology and exert oxygen barrier properties and antibacterial effect on Gram-positive and Gram-negative microorganisms, with modular entity depending of the nanostructured coating composition, reaching up to 88 % reduction of the OTR of the pristine substrate (PE) and inhibition up to 61% and 74% of the *Weizmannia coagulans* and *E. Coli* microorganisms, respectively. Their antimicrobial activity is comparable to most of the systems

reported in literature whose performances have been previously detailed. Moreover, significant oxygen barrier properties have been demonstrated for the proposed hybrid ZnO/GO/MMT coatings, and this represent an additional functional property towards multifunctional coatings, very promising for application in the field of packaging.

4. Conclusion

ZnO NPs with different shape, size and specific surface area were synthesized through hydrothermal and solvothermal methods. The synthesized ZnO NPs shape varies from spherical to hexagonal and platelet-like, with dimension ranging from 10 nm up to about 500 nm, depending on their shape.

The NPs can be dispersed by ultrasonication in aqueous media. By mixing them with GO and GO/MMT water dispersions, they can be easily deposed on flexible substrates by rod coating in order to obtain hybrid ZnO/GO/MMT thin coatings. Indeed, due to the self-assembly ability of GO, GO coatings exhibit high adherence of polymer substrates and flexibility as well as exceptional gas barrier properties; the combination of GO and MMT with ZnO NPs is suited to design hybrid coatings in which the ZnO NPs are well embedded in the thin nanostructured layer.

The effect of the ZnO NPs into the nanostructured hybrid coatings depends on their shape, size and specific surface area, with the highest contribute to oxygen barrier properties related to the platelets-shaped NPs. Coatings composed of 30 wt% of platelets-shaped ZnO NPs, 30 wt% of GO and 40% wt of MMT show OTR values almost comparable to the GO coatings, reaching values of 88 % of reduction of the PE permeability. Moreover, the ZnO/GO/MMT coatings exhibit antibacterial activity towards Gram-positive, Gram-negative microorganisms or both, depending on the NPs shape, size and the coating composition. In particular, the highest performing oxygen barrier coating, ZnO-P30_GO30_MMT40, also shows significant antibacterial effect towards both *E.coli* and *W. coagulans* (about 60% inhibition), evidencing a correlation between oxygen permeability and microbial proliferation. Altogether, results demonstrate that the nanostructured hybrids based on ZnO NPs, GO and MMT are multifunctional monomaterial coatings with gas barrier and antibacterial properties.

CRediT authorship contribution statement

Emre Alp: Writing – original draft, Methodology, Investigation, Conceptualization. **Federico Olivieri:** Writing – review & editing, Writing – original draft, Methodology, Investigation, Conceptualization. **Martina Aulitto:** Writing – original draft, Methodology, Investigation. **Rachele Castaldo:** Writing – review & editing, Writing – original draft, Visualization, Validation, Supervision, Methodology, Investigation, Conceptualization. **Patrizia Contursi:** Writing – original draft, Supervision, Methodology. **Mariacristina Cocca:** Writing – review & editing, Visualization, Methodology, Conceptualization. **Gennaro Gentile:** Writing – review & editing, Visualization, Validation, Methodology, Investigation, Conceptualization.

Declaration of competing interest

The authors declare that they have no known competing financial interests or personal relationships that could have appeared to influence the work reported in this paper.

Acknowledgments

This article is based upon work developed during a Short Term Scientific Missions (STSM) within the framework of the Action “Plastics monitoRIng detectiOn RemedIaTion recovery” - PRIORITY, CA20101, supported by COST (European Cooperation in Science and Technology).

The authors would like to thank Dr. Luciano di Iorio and Prof. Donato Giovannelli for their assistance with the ICP-MS analysis conducted in this research.

Data availability

The raw/processed data required to reproduce these findings cannot be shared at this time as the data also forms part of an ongoing study.

References

[1] D.A.M. Russell, Sustainable (food) packaging–an overview, Food Addit. Contam. Part A. 31 (2014) 396–401.
[2] V. Guillard, S. Gaucel, C. Fornaciari, H. Angellier-Coussy, P. Buche, N. Gontard, The Next Generation of Sustainable Food Packaging to Preserve Our Environment in a Circular Economy Context, Front. Nutr. 5 (2018) 1–13, https://doi.org/10.3389/fnut.2018.00121.
[3] K. Grönman, R. Soukka, T. Järvi-Kääriäinen, J. Katajajuuri, M. Kuisma, H. Koivupuro, M. Ollila, M. Pitkänen, O. Miettinen, F. Silvenius, Framework for sustainable food packaging design, Packag. Technol. Sci. 26 (2013) 187–200.
[4] H. Haghighi, F. Licciardello, P. Fava, H.W. Siesler, A. Pulvirenti, Recent advances on chitosan-based films for sustainable food packaging applications, Food Packag. Shelf Life. 26 (2020) 100551.
[5] K. Marsh, B. Bugusu, Food packaging - Roles, materials, and environmental issues: Scientific status summary, J. Food Sci. 72 (2007) R39–R55, https://doi.org/10.1111/j.1750-3841.2007.00301.x.
[6] Y. Zhan, Y. Meng, Y. Li, C. Zhang, Q. Xie, S. Wei, M. Lavorgna, Z. Chen, Poly(vinyl alcohol)/reduced graphene oxide multilayered coatings: The effect of filler content on gas barrier and surface resistivity properties, Compos. Commun. 24 (2021) 100670, https://doi.org/10.1016/J.COCO.2021.100670.
[7] H.M.C. Azeredo, C.G. Otoni, D.S. Corrêa, O.B.G. Assis, M.R. de Moura, L.H. C. Mattoso, Nanostructured antimicrobials in food packaging—Recent advances, Biotechnol. J. 14 (2019) 1900068.
[8] W. Zhang, J.W. Rhim, Titanium dioxide (TiO2) for the manufacture of multifunctional active food packaging films, Food Packag. Shelf Life. 31 (2022) 100806.
[9] M. Guerritore, F. Olivieri, R. Castaldo, R. Avolio, M. Cocca, M.E. Errico, M.R. Galdi, C. Carfagna, G. Gentile, Recyclable-by-design mono-material flexible packaging with high barrier properties realized through graphene hybrid coatings, Resour. Conserv. Recycl. 179 (2022) 106126, https://doi.org/10.1016/j.resconrec.2021.106126.
[10] M. Toselli, F. Pilati, M. Marini, F. Doghieri, M.G. De Angelis, M. Minelli, Oxygen permeability of novel organic–inorganic coatings: II. Modification of the organic component with a hydrogen-bond forming polymer, Eur. Polym. J. 44 (2008) 3256–3263.
[11] W.S. Jang, I. Rawson, J.C. Grunlan, Layer-by-layer assembly of thin film oxygen barrier, Thin Solid Films 516 (2008) 4819–4825.
[12] R. Cruz-Silva, M. Endo, M. Terrones, Graphene oxide films, fibers, and membranes, Nanotechnol. Rev. 5 (2016) 377–391.
[13] R. Castaldo, G.C. Lama, P. Aprea, G. Gentile, M. Lavorgna, V. Ambrogi, P. Cerruti, Effect of the oxidation degree on self-assembly, adsorption and barrier properties of nano-graphene, Microporous Mesoporous Mater 260 (2018) 102–115, https://doi.org/10.1016/j.micromeso.2017.10.026.
[14] R. Castaldo, R. Avolio, M. Cocca, M.E. Errico, M. Lavorgna, J. Šalplachta, C. Santillo, G. Gentile, Hierarchically porous hydrogels and aerogels based on reduced graphene oxide, montmorillonite and hyper-crosslinked resins for water and air remediation, Chem. Eng. J. (2022) 430, https://doi.org/10.1016/j.cej.2021.133162.
[15] R. Castaldo, G.C. Lama, P. Aprea, G. Gentile, V. Ambrogi, M. Lavorgna, P. Cerruti, Humidity-Driven Mechanical and Electrical Response of Graphene/Cloisite Hybrid Films, Adv. Funct. Mater. 29 (2019) 1–11, https://doi.org/10.1002/adfm.201807744.
[16] M. Zare, K. Namratha, S. Ilyas, A. Sultana, A. Hezam, M.A. Surmeneva, R. A. Surmenev, M.B. Nayan, S. Ramakrishna, S. Mathur, Emerging trends for ZnO nanoparticles and their applications in food packaging, ACS Food Sci. Technol. 2 (2022) 763–781.
[17] P.J.P. Espitia, C.G. Otoni, N.F.F. Soares, Zinc oxide nanoparticles for food packaging applications. Antimicrob. Food Packag, Elsevier, 2016, pp. 425–431.
[18] L.E. Shi, Z.H. Li, W. Zheng, Y.F. Zhao, Y.F. Jin, Z.X. Tang, Synthesis, antibacterial activity, antibacterial mechanism and food applications of ZnO nanoparticles: a review, Food Addit. Contam. Part A. 31 (2014) 173–186.
[19] I. Kim, K. Viswanathan, G. Kasi, S. Thanakkasaranee, K. Sadeghi, J. Seo, ZnO nanostructures in active antibacterial food packaging: preparation methods, antimicrobial mechanisms, safety issues, future prospects, and challenges, Food Rev. Int. 38 (2022) 537–565.
[20] P.J.P. Espitia, N. de F.F. Soares, J.S. dos R. Coimbra, N.J. de Andrade, R.S. Cruz, E. A.A. Medeiros, Zinc oxide nanoparticles: synthesis, antimicrobial activity and food packaging applications, Food Bioprocess Technol 5 (2012) 1447–1464.
[21] A. Stanković, S. Dimitrijević, D. Uskoković, Influence of size scale and morphology on antibacterial properties of ZnO powders hydrothemally synthesized using different surface stabilizing agents, Colloids Surfaces B Biointerfaces 102 (2013) 21–28, https://doi.org/10.1016/j.colsurfb.2012.07.033.

[22] N. Babayevska, Ł. Przysiecka, I. Iatsunskyi, G. Nowaczyk, M. Jarek, E. Janiszewska, S. Jurga, ZnO size and shape effect on antibacterial activity and cytotoxicity profile, Sci. Rep. 12 (2022) 1–13, https://doi.org/10.1038/s41598-022-12134-3.
[23] B. Malhotra, A. Keshwani, H. Kharkwal, Antimicrobial food packaging: Potential and pitfalls, Front. Microbiol. 6 (2015) 144809.
[24] I.A. Channa, J. Ashfaq, S.J. Gilani, A.A. Shah, A.D. Chandio, M.N. bin Jumah, UV blocking and oxygen barrier coatings based on polyvinyl alcohol and zinc oxide nanoparticles for packaging applications, Coatings 12 (2022) 897.
[25] M.A. Johar, R.A. Afzal, A.A. Alazba, U. Manzoor, Photocatalysis and bandgap engineering using ZnO nanocomposites, Adv. Mater. Sci. Eng. 2015 (2015).
[26] P. Amato, M. Muscetta, V. Venezia, M. Cocca, G. Gentile, R. Castaldo, R. Marotta, G. Vitiello, Eco-sustainable design of humic acids-doped ZnO nanoparticles for UVA/light photocatalytic degradation of LLDPE and PLA plastics, J. Environ. Chem. Eng. 11 (2023) 109003, https://doi.org/10.1016/j.jece.2022.109003.
[27] S. Russo, M. Muscetta, P. Amato, V. Venezia, M. Verrillo, R. Rega, S. Lettieri, M. Cocca, R. Marotta, G. Vitiello, Humic substance/metal-oxide multifunctional nanoparticles as advanced antibacterial-antimycotic agents and photocatalysts for the degradation of PLA microplastics under UVA/solar radiation, Chemosphere 346 (2024) 140605.
[28] A. Farazin, M. Mohammadimehr, H. Naeimi, Flexible self-healing nanocomposite based gelatin/tannic acid/acrylic acid reinforced with zinc oxide nanoparticles and hollow silver nanoparticles based on porous silica for rapid wound healing, Int. J. Biol. Macromol. 241 (2023) 124572.
[29] N. Lepot, M.K. Van Bael, H. Van den Rul, J. D'Haen, R. Peeters, D. Franco, J. Mullens, Influence of incorporation of ZnO nanoparticles and biaxial orientation on mechanical and oxygen barrier properties of polypropylene films for food packaging applications, J. Appl. Polym. Sci. 120 (2011) 1616–1623.
[30] S. Shankar, L.F. Wang, J.W. Rhim, Incorporation of zinc oxide nanoparticles improved the mechanical, water vapor barrier, UV-light barrier, and antibacterial properties of PLA-based nanocomposite films, Mater. Sci. Eng. C. 93 (2018) 289–298.
[31] S. Kumar, A. Mudai, B. Roy, I.B. Basumatary, A. Mukherjee, J. Dutta, Biodegradable hybrid nanocomposite of chitosan/gelatin and green synthesized zinc oxide nanoparticles for food packaging, Foods 9 (2020) 1143.
[32] W.C. Liew, I.I. Muhamad, J.W. Chew, K.J. Abd Karim, Synergistic effect of graphene oxide/zinc oxide nanocomposites on polylactic acid-based active packaging film: Properties, release kinetics and antimicrobial efficiency, Int. J. Biol. Macromol. 253 (2023) 127288.
[33] R. Capuano, R. Avolio, R. Castaldo, M. Cocca, G. Gentile, T. Cirillo, A. Nolasco, M. E. Errico, Up-cycling coffee silverskin into biobased functional coatings, J. Clean. Prod. 469 (2024) 143063.
[34] M. Aulitto, R. Castaldo, R. Avolio, M.E. Errico, Y.Q. Xu, G. Gentile, P. Contursi, Sustainable and Green Production of Nanostructured Cellulose by a 2-Step Mechano-Enzymatic Process, Polymers 15 (2023) 1115.
[35] S. Farris, L. Introzzi, J.M. Fuentes-Alventosa, N. Santo, R. Rocca, L. Piergiovanni, Self-assembled pullulan–silica oxygen barrier hybrid coatings for food packaging applications, J. Agric. Food Chem. 60 (2012) 782–790.
[36] M. Aulitto, S. Fusco, S. Bartolucci, C.J. Franzén, P. Contursi, Bacillus coagulans MA-13: a promising thermophilic and cellulolytic strain for the production of lactic acid from lignocellulosic hydrolysate, Biotechnol. Biofuels. 10 (2017) 1–15.
[37] M. Correggia, L. Di Iorio, A.B. Bastianoni, M. Yücel, A. Cordone, D. Giovannelli, Standard Operating Procedure for the analysis of trace elements in hydrothermal fluids by Inductively Coupled Plasma Mass Spectrometry (ICP-MS), Open Res. Eur. 3 (2023) 90.
[38] W.A. Freitas, B.E.C.F. Soares, M.S. Rodrigues, P. Trigueiro, L.M.C. Honorio, R. Pena-Garcia, A.C.S. Alcântara, E.C. Silva-Filho, M.G. Fonseca, M.B. Furtini, Facile synthesis of ZnO-clay minerals composites using an ultrasonic approach for photocatalytic performance, J. Photochem. Photobiol. A Chem. 429 (2022) 113934.
[39] M. Aulitto, S. Fusco, C.J. Franzén, A. Strazzulli, M. Moracci, S. Bartolucci, P. Contursi, Draft Genome Sequence of Bacillus coagulans MA-13, a Thermophilic Lactic Acid Producer from Lignocellulose, Microbiol. Resour. Announc. 8 (2019) 13–15, https://doi.org/10.1128/mra.00341-19.
[40] M. Aulitto, L. Martinez-Alvarez, G. Fiorentino, D. Limauro, X. Peng, P. Contursi, A Comparative Analysis of Weizmannia coagulans Genomes Unravels the Genetic Potential for Biotechnological Applications, Int. J. Mol. Sci. (2022) 23, https://doi.org/10.3390/ijms23063135.
[41] F. Garcia-Ochoa, E. Gomez, V.E. Santos, J.C. Merchuk, Oxygen uptake rate in microbial processes: an overview, Biochem. Eng. J. 49 (2010) 289–307.
[42] R. Krishnamoorthy, J. Athinarayanan, V.S. Periyasamy, M.A. Alshuniaber, G. Alshammari, M.J. Hakeem, M.A. Ahmed, A.A. Alshatwi, Antibacterial mechanisms of zinc oxide nanoparticle against bacterial food pathogens resistant to beta-lactam antibiotics, Molecules 27 (2022) 2489.
[43] A. Sirelkhatim, S. Mahmud, A. Seeni, N.H.M. Kaus, L.C. Ann, S.K.M. Bakhori, H. Hasan, D. Mohamad, Review on zinc oxide nanoparticles: antibacterial activity and toxicity mechanism, Nano-Micro Lett. 7 (2015) 219–242.
[44] E.P.on B.H. (BIOHAZ), Scientific Opinion on the maintenance of the list of QPS biological agents intentionally added to food and feed (2013 update), EFSA J. 11 (2013) 3449.
[45] S. Shankar, L.F. Wang, J.W. Rhim, Incorporation of zinc oxide nanoparticles improved the mechanical, water vapor barrier, UV-light barrier, and antibacterial properties of PLA-based nanocomposite films, Materials Science and Engineering: C 93 (2018) 289–298.
[46] W.C. Liew, I.I. Muhamad, J.W. Chew, K.J. Abd Karim, Synergistic effect of graphene oxide/zinc oxide nanocomposites on polylactic acid-based active packaging film: properties, release kinetics and antimicrobial efficiency, International Journal of Biological Macromolecules 253 (2023) 127288.
[47] I.A. Channa, J. Ashfaq, S.J. Gilani, A.A. Shah, A.D. Chandio, M.N.B. Jumah, UV blocking and oxygen barrier coatings based on polyvinyl alcohol and zinc oxide nanoparticles for packaging applications, Coatings 12 (2022) 897.
[48] H. Rokbani, F. Daigle, A. Ajji, Long-and short-term antibacterial properties of low-density polyethylene-based films coated with zinc oxide nanoparticles for potential use in food packaging, Journal of Plastic Film & Sheeting 35 (2019) 117–134.
[49] D. Valerini, L. Tammaro, F. Di Benedetto, G. Vigliotta, L. Capodieci, R. Terzi, A. Rizzo, Aluminum-doped zinc oxide coatings on polylactic acid films for antimicrobial food packaging, Thin Solid Films 645 (2018) 187–192.
[50] P. Carvalho, P. Sampaio, S. Azevedo, C. Vaz, J.P. Espinós, V. Teixeira, J. O. Carneiro, Influence of thickness and coatings morphology in the antimicrobial performance of zinc oxide coatings, Applied surface science 307 (2014) 548–557.
[51] L. Al-Naamani, S. Dobretsov, J. Dutta, Chitosan-zinc oxide nanoparticle composite coating for active food packaging applications, Innovative Food Science & Emerging Technologies 38 (2016) 231–237.